iScience

CellPress

Article

Impaired Circadian Photoentrainment in *Opn5*-Null Mice

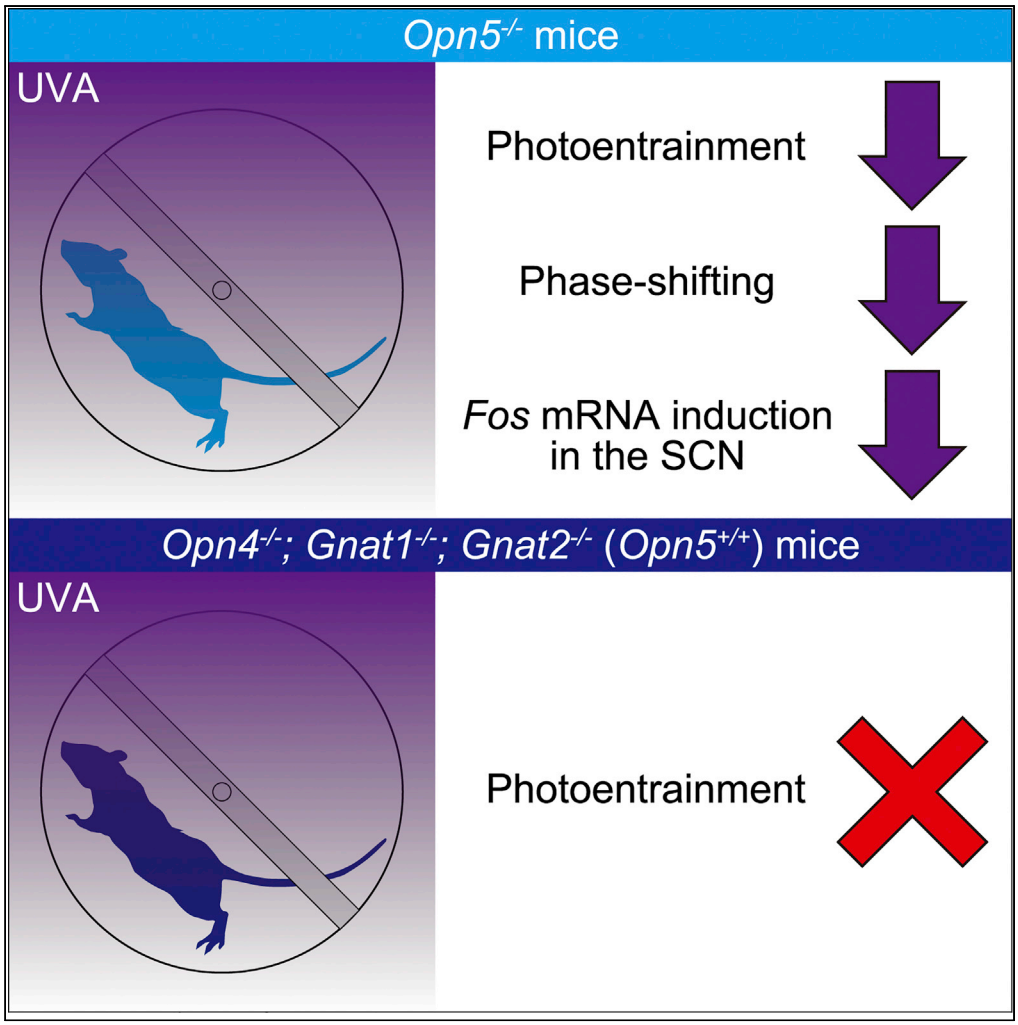

Wataru Ota, Yusuke Nakane, Samer Hattar, Takashi Yoshimura

takashiy@agr.nagoya-u.ac.jp

HIGHLIGHTS

Opn5-null mice show impaired photoentrainment to UVA-light/dark (LD) cycles

Mice lacking melanopsin and functional rods/cones fail to entrain to UVA-LD cycles

Opn5 alone is not sufficient for circadian photoentrainment

Retinal circadian clocks play a possible role in circadian photoentrainment

Ota et al., iScience 6, 299–305
August 31, 2018
https://doi.org/10.1016/j.isci.2018.08.010

iScience

CellPress

Article

Impaired Circadian Photoentrainment in *Opn5*-Null Mice

Wataru Ota,[1,3] Yusuke Nakane,[1,3] Samer Hattar,[5] and Takashi Yoshimura[1,2,3,4,6,*]

SUMMARY

The master circadian pacemaker in mammals resides in the hypothalamic suprachiasmatic nuclei (SCN) and is synchronized to ambient light/dark cycles (i.e., photoentrainment). Melanopsin (Opn4) and classical rod-cone photoreceptors are believed to provide all the photic input necessary for circadian photoentrainment. Although the UVA-sensitive photopigment Opn5 is known to be expressed in retinal ganglion cells, its physiological role remains unclear and a potential role for Opn5 in the photoentrainment of the master clock has not been addressed. Here we report impaired photoentrainment and phase shifting to UVA light in *Opn5*-null mice. However, triple-knockout mice lacking all known functional circadian photoreceptors (i.e., rods, cones, and melanopsin) failed to entrain to UVA-light/dark cycles, despite the presence of Opn5, demonstrating that Opn5 alone is not sufficient for photoentrainment of the SCN clock. Since Opn5 is involved in the regulation of the retinal circadian clock, disrupted retinal function may cause impaired circadian photoentrainment in *Opn5*-null mice.

INTRODUCTION

Circadian rhythms are approximately 24-hr, cell-autonomous biological rhythms observed in virtually all living organisms. The mammalian circadian pacemaker resides in the hypothalamic suprachiasmatic nuclei (SCN). Daily physiological and behavioral activity patterns are regulated by the SCN, which is synchronized to ambient light/dark (LD) cycles via direct connections from retinal ganglion cells in the retina. Thus, circadian photoentrainment enables organisms to enhance their fitness by anticipating daily changes in food availability and predator activity. Melanopsin (Opn4) and classical rod-cone photoreceptive systems are widely believed to provide all photic input required for circadian photoentrainment (Hattar et al., 2003; Panda et al., 2003), and a potential role for other photopigments has not been addressed. Opn5 is a deep brain photopigment that regulates seasonal reproduction in birds (Nakane et al., 2010, 2014; Yamashita et al., 2010). In mammals, Opn5 is expressed in selected retinal ganglion cells and exhibits an absorption maximum in the UVA range (λ_{max} = 380 nm) (Kojima et al., 2011; Yamashita et al., 2014). Although mammalian Opn5 has been demonstrated to be involved in the photoentrainment of local circadian clocks in the retina and the cornea, its involvement in photoentrainment of the SCN remains unclear (Buhr et al., 2015).

RESULTS AND DISCUSSION

Generation of Mice Deficient in Opn5 and Classical Rod-Cone Photoreceptors

To assess the physiological function of mammalian Opn5 *in vivo*, we generated *Opn5*-null (*Opn5*$^{-/-}$) mice (Figures 1A–1D). Since mice also possess a UVA-sensitive cone opsin (Opn1sw; λ_{max} = 360 nm), we generated mice deficient in Opn5 and classical rod-cone photoreceptors (*Opn5*$^{-/-}$*; rd1/rd1*) by breeding *Opn5*-null mice with CBA/J mice harboring the retinal degeneration (*rd1*) mutation. Because the genetic background of *Opn5*-null mice was C57BL/6J, F2 hybrids of the parental strains were used to minimize the effect of genetic background, as suggested by the Jackson Laboratory. To examine the effects of *Opn5* deficiency and the *rd1* mutation on retinal morphology, we performed immunohistochemistry and analyzed the expression of different opsins. Information about the antibodies used is given in Table S1. The retina of *Opn5*-null mice was indistinguishable from that of wild-type (WT) mice, and immunopositive signals for rod (Rho) and cone (Opn1sw; Opn1mw) opsins and melanopsin (Opn4) were observed (Figure 1E). By contrast, although the *rd1* mutation caused severe retinal degeneration and abolished the rod-cone photoreceptor layer, the retinal ganglion cell layer was intact and melanopsin expression was clearly observed in both *rd1/rd1* and *Opn5*$^{-/-}$*; rd1/rd1* mutants (Figure 1E). Note that we have generated several antibodies against Opn5, but none of them were specific; therefore, we were unable to examine the expression of Opn5 in the different mutant mice.

[1]Laboratory of Animal Integrative Physiology, Graduate School of Bioagricultural Sciences, Nagoya University, Nagoya 464-8601, Japan

[2]Avian Bioscience Research Center, Graduate School of Bioagricultural Sciences, Nagoya University, Nagoya 464-8601, Japan

[3]Institute of Transformative Bio-Molecules (WPI-ITbM), Nagoya University, Nagoya 464-8601, Japan

[4]Division of Seasonal Biology, National Institute for Basic Biology, Okazaki 444-8585, Japan

[5]Section on Light and Circadian Rhythms, National Institute of Mental Health, National Institutes of Health, Bethesda, MD 20892, USA

[6]Lead Contact

*Correspondence: takashiy@agr.nagoya-u.ac.jp

https://doi.org/10.1016/j.isci.2018.08.010

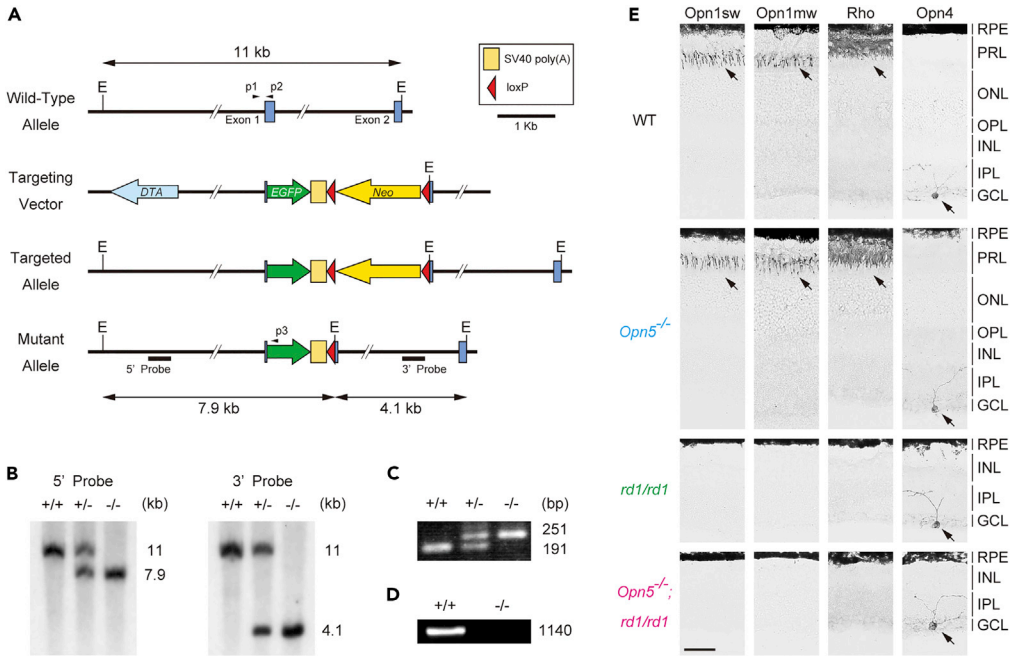

Figure 1. Generation of *Opn5*$^{-/-}$ Mice, and Histological Analysis of the Retina

(A) Physical map of the wild-type *Opn5* locus, targeting construct, targeted allele before Cre-mediated recombination, and disrupted *Opn5* locus. The targeting vector was designed to excise a part of *Opn5* exon 1 and insert *EGFP* in-frame with the start codon of *Opn5*, followed by an SV40 poly(A) tail. The SV40 poly(A) tail halts the transcription of the full-length *Opn5* transcript, resulting in *Opn5* deficiency. The 5′ and -3′ probes used for screening targeted embryonic stem (ES) clones and mouse genotypes are represented by the black bars. PCR primers used for mouse genotyping (p1–3) are shown as arrowheads. E, *Eco*RV; *Neo*, neomycin resistance gene; *DTA*, diphtheria toxin.

(B) Southern blot analysis of genomic DNA from *Opn5*$^{+/+}$, *Opn5*$^{+/-}$, and *Opn5*$^{-/-}$ mice, hybridized with indicated probes. If homologous recombination was successful, the fragment corresponding to the wild-type *Opn5* allele (11 kb) is replaced by a smaller fragment representing the recombined mutant allele (7.9 or 4.1 kb).

(C) PCR genotyping of genomic DNA. Amplicons corresponding to the wild-type (191 bp) and targeted allele (251 bp) are indicated.

(D) Absence of *Opn5* mRNA in the retina was confirmed by RT-PCR.

(E) Immunohistochemistry of photopigments in the retina of WT, *Opn5*$^{-/-}$, *rd1/rd1*, and *Opn5*$^{-/-}$; *rd1/rd1* mice, respectively. Arrows indicate immunopositive signals. RPE, retinal pigment epithelium; PRL, photoreceptor layer; ONL, outer nuclear layer; OPL, outer plexiform layer; INL, inner nuclear layer; IPL, inner plexiform layer; GCL, ganglion cell layer. Scale bar: 50 μm.

See also Figure S1A and Table S1.

Impaired Re-Entrainment to UVA-LD Cycles in *Opn5*-Null Mice

We then compared photoentrainment to UVA-LD cycles in WT mice, *Opn5*$^{-/-}$ and *rd1/rd1* single mutant mice, and *Opn5*$^{-/-}$; *rd1/rd1* double mutant mice. Absorption spectra of the retinal photopigments present in these mice are illustrated in Figure S1A. Mice were initially kept under white-LD cycles and then transferred to UVA-LD cycles (λ_p = 365 nm, Figure S1B); wheel-running activity was recorded to measure entrainment (Figure 2A). The intensity of the UVA light was decreased every 2–10 weeks, concomitant with a 2-hr advance of the LD cycle, as described previously (Butler and Silver, 2011). Entrainment to the advanced UVA-LD cycles was determined by a transient interval of a free-running rhythm with a period shorter than 24 hr, which was then followed by a 24-hr rhythm with a stable phase angle of entrainment.

Double mutant mice (*Opn5*$^{-/-}$; *rd1/rd1*) required more days for re-entrainment to new UVA-LD cycles than WT mice (Figure 2B), whereas the single mutants (*Opn5*$^{-/-}$ and *rd1/rd1*) exhibited intermediate phenotypes (Figure 2B) (e.g., WT: ~12 days, *rd1/rd1*: ~20 days, *Opn5*$^{-/-}$: ~23 days, *Opn5*$^{-/-}$; *rd1/rd1*: ~30 days at a log photon flux of 12.7). Half-maximal intensities (I_{50}) for entrainment were higher for single and double mutant mice than for WT mice (Figures 2C and 2D). Although differences in the free-running period can affect the duration and light intensity required for re-entrainment, the free-running period of

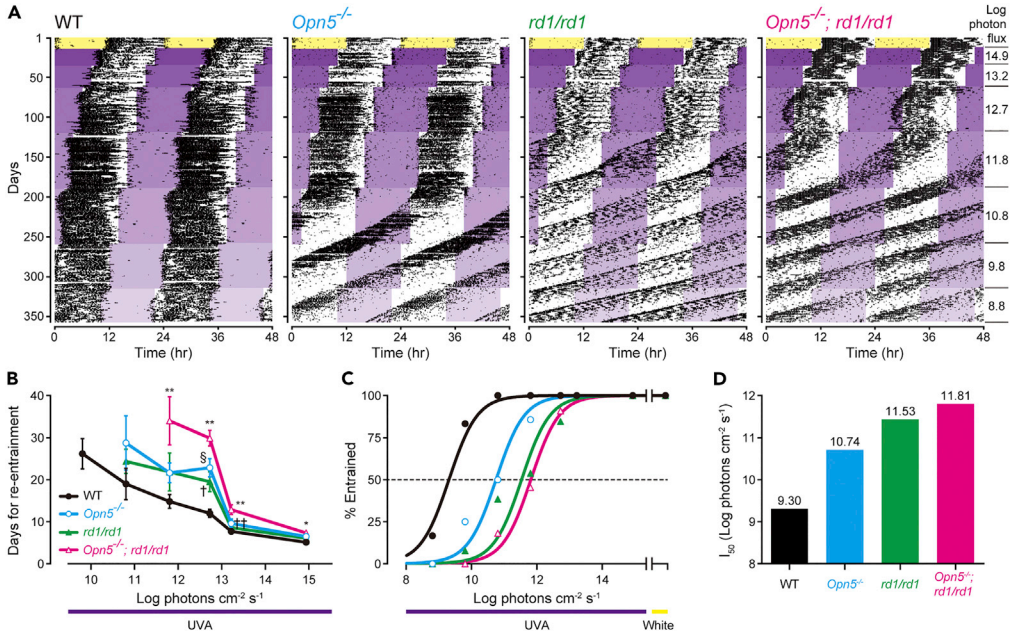

Figure 2. Impaired Circadian Photoentrainment to UVA-LD Cycles in *Opn5*$^{-/-}$, *rd1/rd1*, and *Opn5*$^{-/-}$; *rd1/rd1* Mice

(A) Representative double-plotted actograms of WT, *Opn5*$^{-/-}$, *rd1/rd1*, and *Opn5*$^{-/-}$; *rd1/rd1* mice. The vertical and horizontal axes indicate the number of recorded days and the time of day over 2 days, respectively. Yellow and purple represent white and UVA light, respectively. The log photon flux of UVA light (log photons cm^{-2} s^{-1}) is indicated on the right.

(B) Days required for re-entrainment to a new LD cycle. *, WT versus *Opn5*$^{-/-}$; *rd1/rd1*. §, WT versus *Opn5*$^{-/-}$. †, *rd1/rd1* versus *Opn5*$^{-/-}$; *rd1/rd1*. Values represent the mean ± SEM. Single symbol, $p < 0.05$; double symbol, $p < 0.01$ (one-way ANOVA followed by Scheffé's post-hoc test; n = 4–13).

(C) Percentage of animals entrained at each step. To calculate the half-maximal intensity (I_{50}), a three-parameter logistic function (sigmoidal dose-response) was fitted to intensity-response relationships using GraphPad Prism.

(D) I_{50} for the entrainment of each genotype.

See also Figures S1 and S2.

all 4 genotypes did not differ significantly (Figure S2). Together, these results demonstrated that *Opn5*$^{-/-}$ and *rd1/rd1* mice exhibit significantly slower rates of re-entrainment to UVA-LD cycles than WT mice.

Although *Opn5*$^{-/-}$; *rd1/rd1* mice exhibited severe impairment in circadian photoentrainment, they were able to entrain to the higher intensity UVA-LD cycles, suggesting the involvement of additional photopigments. In the *rd1/rd1* retina, most rods degenerate rapidly (within the first week after birth) and all rods disappear completely by about 7 weeks of age. By contrast, cones degenerate much more slowly, with some surviving for at least 18 months (Carter-Dawson et al., 1978). The involvement of UVA-sensitive cones in circadian photoentrainment is well established (van Oosterhout et al., 2012; Yoshimura and Ebihara, 1998). Therefore, it is possible that the remaining UVA-sensitive cone opsins and/or melanopsin may mediate UVA-dependent circadian photoentrainment in *Opn5*$^{-/-}$; *rd1/rd1* mice.

Impaired Phase Shifting and *Fos* Induction to UVA Light Pulses in *Opn5*-Null Mice

To further evaluate the ability of *Opn5*-null mice to respond to light for circadian functions, we examined the effect of phase-shifting light pulses under constant darkness (Figure 3). A single 15-min light pulse was given 4 hr after activity onset (i.e., circadian time 16). Retinal degenerate (*rd1/rd1*) mice showed decreased phase shifts to both UVA and orange light pulses (λ_p = 602 nm, Figure S1B) compared with WT mice (Figures 3A–3D). This is most likely due to the loss of classical photoreceptors, whose contribution to irradiance encoding and regulation of circadian rhythms is well known (Altimus et al., 2010; Lall et al., 2010; van Diepen et al., 2013; van Oosterhout et al., 2012; Yoshimura and Ebihara, 1996, 1998). Although *Opn5*$^{-/-}$ mice showed impaired phase shifting to UVA light pulses (Figures 3A and 3C), they showed normal phase shifting to orange light pulses (Figures 3B and 3D), indicating that impaired photoresponses observed in *Opn5*$^{-/-}$ mice are UVA light specific.

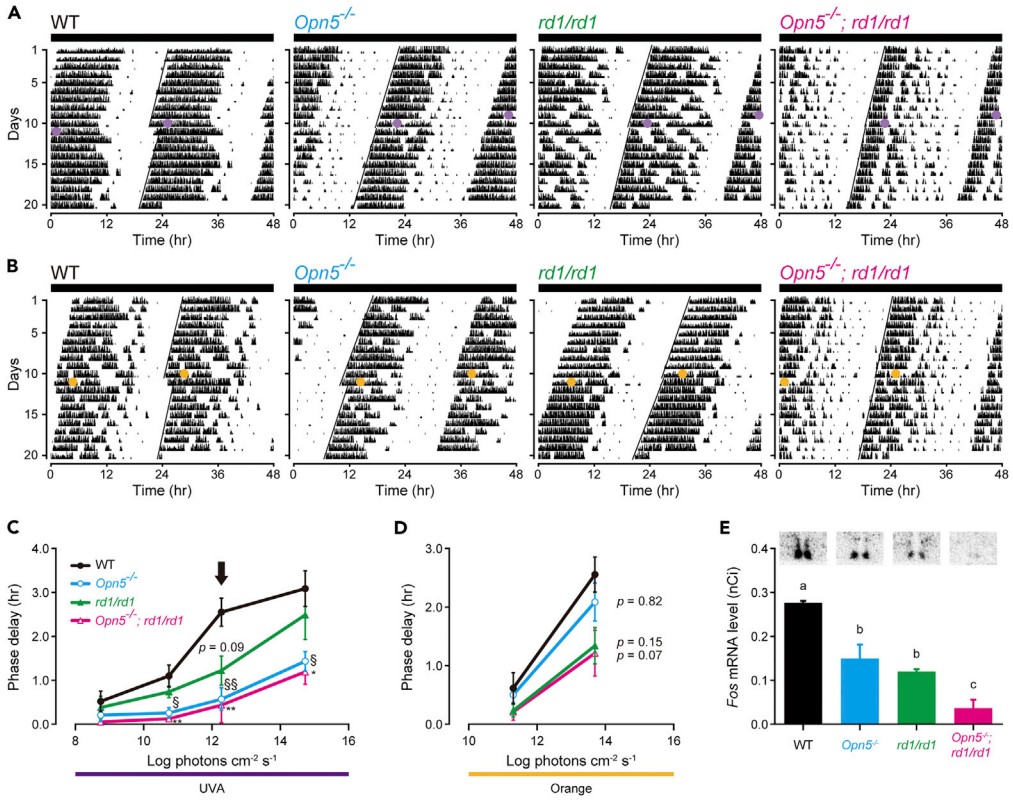

Figure 3. Impaired Phase Shifting and *Fos* Induction to a UVA Light Pulse in *Opn5*$^{-/-}$, *rd1/rd1*, and *Opn5*$^{-/-}$; *rd1/rd1* Mice

(A and B) Effects of a single 15-min UVA light pulse (purple filled circles, λ_p = 365 nm, 12.3 log photons cm^{-2} s^{-1}) (A) and orange-light pulse (orange filled circles, λ_p = 602 nm, 13.7 log photons cm^{-2} s^{-1}) (B) on wheel-running activity rhythms. Representative double-plotted actograms of each genotype are shown. Eye-fitted lines were drawn using activity onset as a reference point.

(C and D) Irradiance-response relationship of circadian phase shifts by UVA (C) and orange-light (D) pulses. The magnitude of the phase shift was determined by eye-fitted lines as shown in (A) and (B). *, WT versus *Opn5*$^{-/-}$; *rd1/rd1*. §, WT versus *Opn5*$^{-/-}$. Values represent the mean ± SEM. Single symbol, $p < 0.05$; double symbols, $p < 0.01$ (one-way ANOVA followed by Scheffé's post-hoc test; n = 5–9).

(E) Densitometric quantification of *Fos* mRNA expression in the SCN induced by a single UVA light pulse at the intensity indicated by the black arrow in (C) (12.3 log photons cm^{-2} s^{-1} for 15-min). Values represent the mean ± SEM. $p < 0.05$ (one-way ANOVA followed by Scheffé's post-hoc test; n = 4–5). Representative autoradiograms are shown at the top. See also Figures S1 and S2.

We also examined the induction of neuronal activation marker, *Fos* mRNA, in the SCN by UVA light (single 15-min pulse at a log photon flux of 12.3 cm^{-2} s^{-1}). These results showed that UVA-dependent *Fos* induction was significantly decreased in *Opn5*$^{-/-}$ and *rd1/rd1* single mutant mice, as well as in *Opn5*$^{-/-}$; *rd1/rd1* double mutants (Figure 3E). However, the phenotype was much more severe in double mutant mice (*Opn5*$^{-/-}$; *rd1/rd1*) than in the single mutants (*Opn5*$^{-/-}$ and *rd1/rd1*) and correlates well with our phase shifting results in Figure 3C. All together, these results demonstrated that *Opn5*$^{-/-}$ mice have decreased photosensitivity to UVA light.

Opn4$^{-/-}$; *Gnat1*$^{-/-}$; *Gnat2*$^{-/-}$ Mice Lack the Ability to Photoentrain to UVA-LD Cycles

Previous studies have shown that mice deficient in melanopsin and rod-cone photoreceptors (e.g., *Opn4*$^{-/-}$; *rd1/rd1* double mutant mice and *Opn4*$^{-/-}$; *Gnat1*$^{-/-}$; *Cnga3*$^{-/-}$ [melanopsin; guanine nucleotide-binding protein α transducin 1; cyclic nucleotide-gated channel α3, respectively] triple-knockout [TKO] mice) failed to entrain to white-LD cycles; therefore, melanopsin and classical rod-cone photoreceptive systems are widely believed to account for all photic input required for circadian photoentrainment (Hattar et al., 2003; Panda et al., 2003). However, these studies used relatively dim white light (100–800 lx) (Hattar et al., 2003;

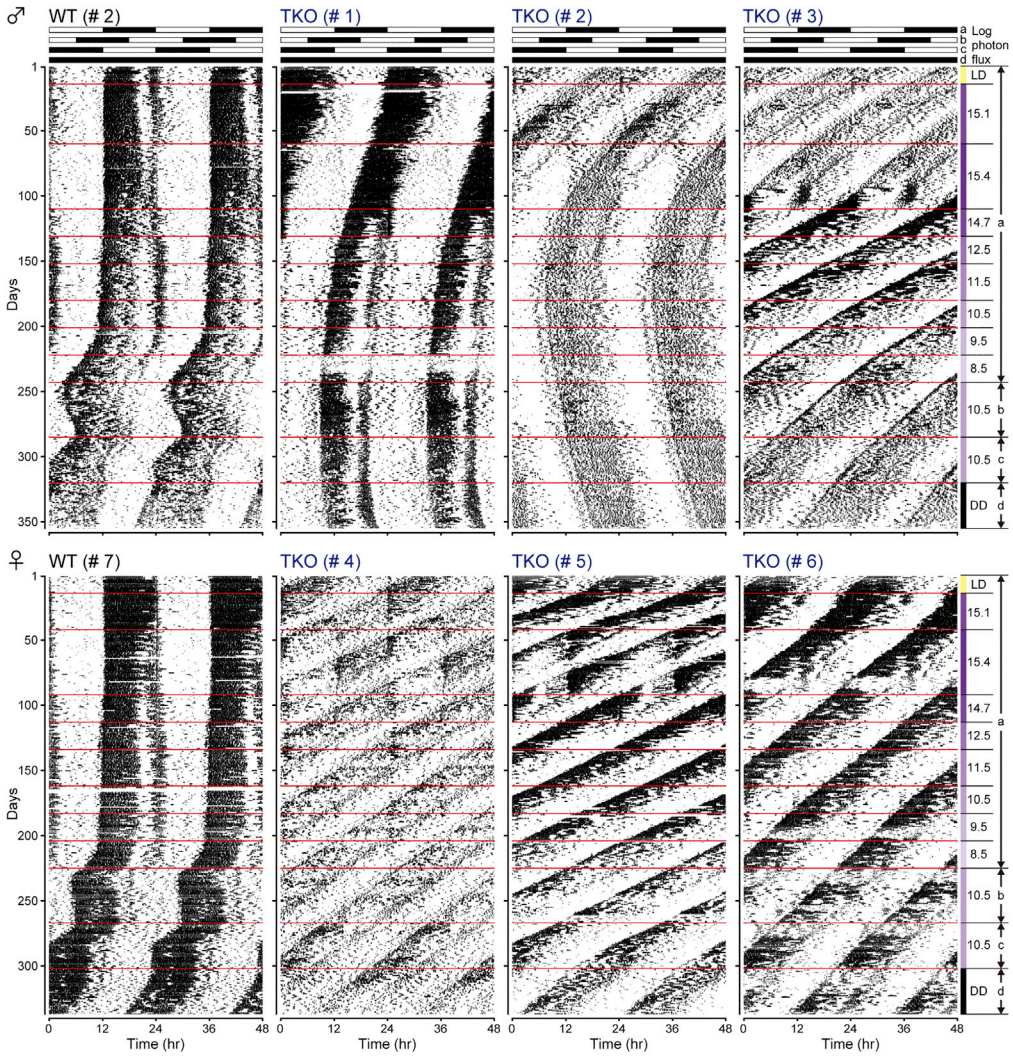

Figure 4. Photoentrainment Analysis of *Opn4*$^{-/-}$; *Gnat1*$^{-/-}$; *Gnat2*$^{-/-}$ Mice

Representative double-plotted actograms of WT and *Opn4*$^{-/-}$; *Gnat1*$^{-/-}$; *Gnat2*$^{-/-}$ TKO mice. The vertical and horizontal axes indicate the number of recorded days and the time of day over 2 days, respectively. Yellow, purple, and black bars on the right indicate different lighting conditions: white-LD cycles, UVA-LD cycles, and constant darkness (DD), respectively. The log photon flux of UVA light (log photons cm^{-2} s^{-1}) is also marked on the right. The timing of different LD cycles is illustrated at the top, and the assigned letter (a–d) for each LD cycle corresponds to the letter shown on the right. The red lines indicate when lighting conditions were changed. See also Figure S1.

Panda et al., 2003). The illuminance under direct sunlight is approximately 100,000 lx, whereas that of sunrise or sunset on a clear day is approximately 400 lx. Thus, it is possible that the illuminance (i.e., 100–800 lx) and/or wavelengths (i.e., white light but not UVA light) used in these previous studies were not sufficient to stimulate Opn5. We therefore examined circadian photoentrainment to UVA-LD cycles in *Opn4*$^{-/-}$; *Gnat1*$^{-/-}$; *Gnat2*$^{-/-}$ TKO mice (Gnat1/2: guanine nucleotide-binding protein α transducin 1/2), which have mutations in all known circadian photoreceptor pathways (Figure S1A). WT and TKO mice were initially kept under white-LD cycles and then transferred to UVA-LD cycles. The intensity of UVA light was adjusted every 3–7 weeks. WT mice could entrain to white- and UVA-LD cycles, except at very low intensities of UVA light (log photon flux of 8.5–9.5 cm^{-2} s^{-1}); however, TKO mice failed to entrain to LD cycles of white light and all intensities of UVA light (Figure 4). Although 2 of 6 TKO mice (#1 and #2) showed free-running periods close to 24 hr, they failed to entrain to advanced UVA-LD cycles (Figure 4). These results demonstrated that the UVA-sensitive photopigment Opn5 alone is not sufficient for photoentrainment of the circadian pacemaker.

Conclusions

In the present study, we demonstrated impaired photoentrainment to UVA light in *Opn5*-null mice. However, *Opn4*$^{-/-}$; *Gnat1*$^{-/-}$; *Gnat2*$^{-/-}$ TKO mice that lack melanopsin and functional rod-cone photoreceptors, but still possess Opn5, failed to photoentrain to LD cycles of both white and UVA light. This means that Opn5 is required for maximum UVA sensitivity, but it alone is not sufficient for entrainment to UVA-LD cycles. Although it is possible that Gnat1 and/or Gnat2 are involved in the phototransduction of Opn5, this seems unlikely, since they are thought to be expressed in different cell types, with Opn5 being expressed in retinal ganglion cells and Gnat1/2 in rod and cone photoreceptors, respectively (Buhr et al., 2015). The mammalian retina itself has a local circadian clock (Buhr and Van Gelder, 2014; Tosini and Menaker, 1996), which is photoentrainable *in vivo* and *ex vivo* and does not require the SCN. Photoentrainment of the retinal clock is mediated by Opn5 and not by melanopsin or rod-cone photoreceptors (Buhr et al., 2015). Thus, the retinal circadian clock is likely to be disrupted in *Opn5*$^{-/-}$ mice. Many retinal functions are known to be under the control of the circadian clock. For example, photoreceptors undergo daily cycles of renewal and shedding of outer segment disc membranes, which are fundamental for the maintenance of photoreceptor health (La Vail, 1976). Rod and cones are anatomically coupled by gap junctions, and the retinal circadian clock controls the extent and strength of rod-cone electrical coupling, leading to changes in retinal sensitivity between the daytime and nighttime (Ribelayga et al., 2008). Furthermore, disruption of the retinal circadian clock has been demonstrated to result in abnormal retinal transcriptional responses to light and defective inner retinal electrical responses to light (Storch et al., 2007). It is therefore plausible that the impaired photoentrainment we observed in *Opn5*-null mice is caused by disruption of the retinal circadian clock.

Although Opn5 is expressed in retinal ganglion cells, it alone is not sufficient for photoentrainment of the circadian pacemaker in the SCN. However, remarkably, Opn5 still contributes to circadian light responses even in the presence of functional rods, cones, and melanopsin light responses.

Limitations of the Study

Our study focused primarily on behavioral analysis of circadian locomotor activity of various mutant mice (except Figures 1 and 3E). Therefore, we do not fully understand the underlying mechanism of impaired photoentrainment and phase shifting in Opn5-null mice. Further molecular analysis of the retina of Opn5-null mice might be required in future studies to characterize this mechanism.

METHODS

All methods can be found in the accompanying Transparent Methods supplemental file.

SUPPLEMENTAL INFORMATION

Supplemental Information includes Transparent Methods, two figures, and one table and can be found with this article online at https://doi.org/10.1016/j.isci.2018.08.010.

ACKNOWLEDGMENTS

We thank Dr. Kathy Tamai for comments on the manuscript, Mr. Kousuke Okimura for technical support, Dr. Willem J. DeGrip for the Rho antibody, and Dr. Keisuke Ikegami for helpful discussions. We also thank the Nagoya University Radioisotope Center for use of their facilities. This work was supported by the Funding Program for Next Generation World Leading Researchers (NEXT Program) initiated by the Council for Science and Technology Policy (CSTP) (LS055), JSPS KAKENHI "Grant-in-Aid for Specially Promoted Research" (Grant Number 26000013), Human Frontier Science Program (RGP0030/2015), Grant-in-Aid for JSPS Fellows (14J03915), and Program for Leading Graduate Schools "Integrative Graduate Education and Research in Green Natural Sciences (IGER)," MEXT, Japan. WPI-ITbM is supported by World Premier International Research Center Initiative (WPI), MEXT, Japan.

AUTHOR CONTRIBUTIONS

T.Y. conceived and directed the work; W.O. and Y.N. performed research; S.H. provided new materials; W.O. and T.Y. analyzed data; all authors discussed the results and commented on the manuscript; W.O. and T.Y. wrote the paper.

DECLARATION OF INTERESTS

The authors declare no competing interests.

Received: December 21, 2015
Revised: July 25, 2018
Accepted: August 10, 2018
Published: August 31, 2018

REFERENCES

Altimus, C.M., Güler, A.D., Alam, N.M., Arman, A.C., Prusky, G.T., Sampath, A.P., and Hattar, S. (2010). Rod photoreceptors drive circadian photoentrainment across a wide range of light intensities. Nat. Neurosci. *13*, 1107–1112.

Buhr, E.D., and Van Gelder, R.N. (2014). Local photic entrainment of the retinal circadian oscillator in the absence of rods, cones, and melanopsin. Proc. Natl. Acad. Sci. USA *111*, 8625–8630.

Buhr, E.D., Yue, W.W.S., Ren, X., Jiang, Z., Liao, H.R., Mei, X., Vemaraju, S., Nguyen, M.T., Reed, R.R., Lang, R.A., et al. (2015). Neuropsin (OPN5)-mediated photoentrainment of local circadian oscillators in mammalian retina and cornea. Proc. Natl. Acad. Sci. USA *112*, 13093–13098.

Butler, M.P., and Silver, R. (2011). Divergent photic thresholds in the non-image-forming visual system: entrainment, masking and pupillary light reflex. Proc. Biol. Sci. *278*, 745–750.

Carter-Dawson, L.D., LaVail, M.M., and Sidman, R.L. (1978). Differential effect of the *rd* mutation on rods and cones in the mouse retina. Invest. Ophthalmol. Vis. Sci. *17*, 489–498.

Hattar, S., Lucas, R.J., Mrosovsky, N., Thompson, S., Douglas, R.H., Hankins, M.W., Lem, J., Biel, M., Hofmann, F., Foster, R.G., et al. (2003). Melanopsin and rod-cone photoreceptive systems account for all major accessory visual functions in mice. Nature *424*, 76–81.

Kojima, D., Mori, S., Torii, M., Wada, A., Morishita, R., and Fukada, Y. (2011). UV-sensitive photoreceptor protein OPN5 in humans and mice. PLoS One *6*, e26388.

La Vail, M.M. (1976). Survival of some photoreceptor cells in albino rats following long-term exposure to continuous light. Invest. Ophthalmol. *15*, 64–70.

Lall, G.S., Revell, V.L., Momiji, H., Al Enezi, J., Altimus, C.M., Güler, A.D., Aguilar, C., Cameron, M.A., Allender, S., Hankins, M.W., et al. (2010). Distinct contributions of rod, cone, and melanopsin photoreceptors to encoding irradiance. Neuron *66*, 417–428.

Nakane, Y., Ikegami, K., Ono, H., Yamamoto, N., Yoshida, S., Hirunagi, K., Ebihara, S., Kubo, Y., and Yoshimura, T. (2010). A mammalian neural tissue opsin (Opsin 5) is a deep brain photoreceptor in birds. Proc. Natl. Acad. Sci. USA *107*, 15264–15268.

Nakane, Y., Shimmura, T., Abe, H., and Yoshimura, T. (2014). Intrinsic photosensitivity of a deep brain photoreceptor. Curr. Biol. *24*, R596–R597.

Panda, S., Provencio, I., Tu, D.C., Pires, S.S., Rollag, M.D., Castrucci, A.M., Pletcher, M.T., Sato, T.K., Wiltshire, T., Andahazy, M., et al. (2003). Melanopsin is required for non-image-forming photic responses in blind mice. Science *301*, 525–527.

Ribelayga, C., Cao, Y., and Mangel, S.C. (2008). The circadian clock in the retina controls rod-cone coupling. Neuron *59*, 790–801.

Storch, K.F., Paz, C., Signorovitch, J., Raviola, E., Pawlyk, B., Li, T., and Weitz, C.J. (2007). Intrinsic circadian clock of the mammalian retina: importance for retinal processing of visual information. Cell *130*, 730–741.

Tosini, G., and Menaker, M. (1996). Circadian rhythms in cultured mammalian retina. Science *272*, 419–421.

van Diepen, H.C., Ramkisoensing, A., Peirson, S.N., Foster, R.G., and Meijer, J.H. (2013). Irradiance encoding in the suprachiasmatic nuclei by rod and cone photoreceptors. FASEB J. *27*, 4204–4212.

van Oosterhout, F., Fisher, S.P., van Diepen, H.C., Watson, T.S., Houben, T., VanderLeest, H.T., Thompson, S., Peirson, S.N., Foster, R.G., and Meijer, J.H. (2012). Ultraviolet light provides a major input to non-image-forming light detection in mice. Curr. Biol. *22*, 1397–1402.

Yamashita, T., Ohuchi, H., Tomonari, S., Ikeda, K., Sakai, K., and Shichida, Y. (2010). Opn5 is a UV-sensitive bistable pigment that couples with Gi subtype of G protein. Proc. Natl. Acad. Sci. USA *107*, 22084–22089.

Yamashita, T., Ono, K., Ohuchi, H., Yumoto, A., Gotoh, H., Tomonari, S., Sakai, K., Fujita, H., Imamoto, Y., Noji, S., et al. (2014). Evolution of mammalian Opn5 as a specialized UV-absorbing pigment by a single amino acid mutation. J. Biol. Chem. *289*, 3991–4000.

Yoshimura, T., and Ebihara, S. (1996). Spectral sensitivity of photoreceptors mediating phase-shifts of circadian rhythms in retinally degenerate CBA/J (*rd/rd*) and normal CBA/N (+/+) mice. J. Comp. Physiol. A *178*, 797–802.

Yoshimura, T., and Ebihara, S. (1998). Decline of circadian photosensitivity associated with retinal degeneration in CBA/J-*rd/rd* mice. Brain Res. *779*, 188–193.

ISCI, Volume *6*

Supplemental Information

Impaired Circadian Photoentrainment in *Opn5*-Null Mice

Wataru Ota, Yusuke Nakane, Samer Hattar, and Takashi Yoshimura

Supplemental Information

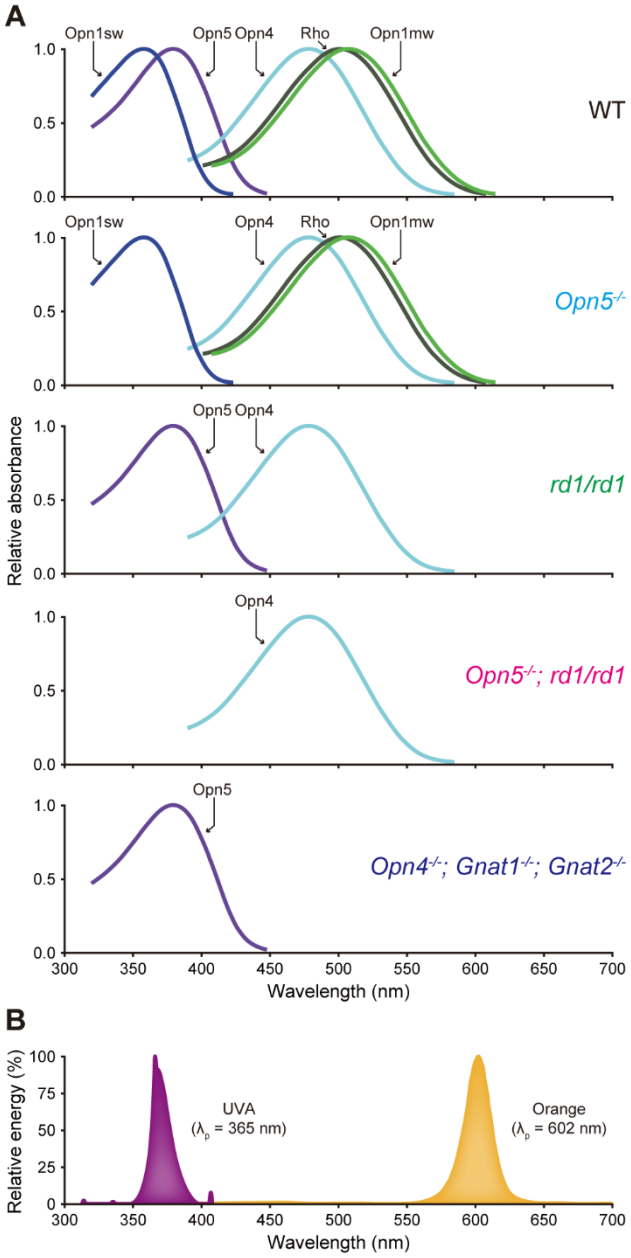

Figure S1. Absorption spectra of retinal photopigments for each genotype, and spectral profiles of light sources used in this study. Related to Figures 1E, 2, 3 and 4.

(A) Schematic diagram of the absorption spectra of the retinal photopigments in the mutant mice used in this study. Modified from Kojima et al. (Kojima et al., 2011). (B) Schematic diagram of the spectral profile of the UVA and orange light sources used in this study. The UVA light source is a fluorescent lamp (Philips), and the orange light source is a light-emitting diode (LED) (Beamtec). Values are shown as relative energy (%).

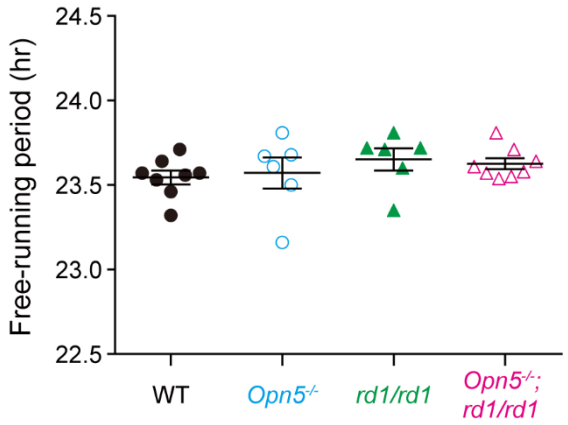

Figure S2. Free-running period of wild type and mutant mouse strains used in this study. Related to Figures 2 and 3.

Values represent the mean ± SEM. No significant differences were observed between genotypes (p > 0.05, one-way ANOVA followed by Scheffé's post-hoc test; n = 6–8).

Name	Manufacturer	Product number	Dilution	Host	Monoclonal/ Polyclonal
Opn1sw	Santa Cruz	sc-14363	1:10000	Goat	Polyclonal
Opn1mw	Chemicon	AB5405	1:8000	Rabbit	Polyclonal
Rho	Dr. Willem J. DeGrip (Schalken and DeGrip, 1986)	CERN886	1:500	Rabbit	Polyclonal
Opn4	Advanced Targeting Systems	AB-N38	1:10000	Rabbit	Polyclonal

Table S1. Antibodies used in this study. Related to Figure 1E.

Transparent Methods

Animals

Male and female F2 progeny generated by intercrosses between *Opn5*$^{-/-}$ mice (C57BL/6J background) and *rd1/rd1* mice (CBA/J strain) were used in this study. *Opn4*$^{-/-}$*; Gnat1*$^{-/-}$*; Gnat2*$^{-/-}$ mice (hybrids between C57BL/6N and 129S strain) were also used in this study. All animals were kept in a controlled environment (white-LD cycle [12/12-hr]; room temperature 22–24°C) until experiments were performed. Food and water were provided *ad libitum*. All animal procedures in this study were approved by the Animal Experiment Committee of Nagoya University.

Generation of *Opn5*-null mice

We manipulated the murine *Opn5* locus by targeted replacement of the *Opn5* gene with a cDNA encoding EGFP (Clontech) (Figure 1A). In the targeting construct, the *EGFP* gene replaces 127 bp of the first exon of *Opn5* starting from the translational start site. Genomic fragments flanking the murine *Opn5* gene were used to generate the *Opn5* targeting vector. Following homologous recombination and isolation of ES cell clones that harbored the expected construct (replacement of *Opn5* by *EGFP*), the *Neo* gene flanked by two loxP sites was then excised. The targeted ES cell clones were injected into blastocysts to generate chimeric mice. Germline transmission of the mutant allele yielded heterozygous mutant *Opn5*$^{+/-}$ mice, which were intercrossed to generate homozygous *Opn5*$^{-/-}$ mice. Because we used C57BL/6J-derived ES cells, the genetic background of *Opn5*-null mice was C57BL/6J. Primers used for genotyping were as follows (see also Figure 1A and 1C):

p1, 5’-ggtgaacatctctccactag-3’
p2, 5’-ggtagggcagtgtggttcaa-3’
p3, 5’-ctgaacttgtggccgtttac-3’

Deficiency of *Opn5* mRNA was examined by RT-PCR. Primers for RT-PCR were designed at exons 1 and 7 as follows:

forward, 5’-atggccttgaaccacactgccctacctcag-3’
reverse, 5’-aggtgcttatttcttgccacagtcaccatc-3’

Immunohistochemistry

Mice were deeply anesthetized with isoflurane and perfused with saline followed by neutral buffered formalin (NBF). Brains were removed, post-fixed for 24 hr in NBF and soaked in 20% sucrose in 0.1

M phosphate buffer (PB, pH 7.4) for 24 hr. The brains were then frozen using dry ice, and coronal frozen sections (20-μm thickness) were prepared using a cryostat. After air-drying, sections were placed in 0.1 M phosphate-buffered saline (PBS, pH 7.4). The sections were soaked in antigen retrieval solution (Histo VT One, Nacalai Tesque), heated in a microwave for 7 min, and quenched for 1 hr at room temperature (RT, ~25°C). Sections were washed in 0.1 M PBS, and endogenous peroxidase activity was blocked with 0.03% H_2O_2 in 0.1 M PBS at RT. The samples were then washed in 0.1 M PBS, followed by a wash in 0.1 M PBS supplemented with 0.3% Triton X-100 (PBST; pH 7.4), and incubated in blocking solution (1.5% normal goat or rabbit serum in 0.1 M PBST) at RT. Sections were then incubated with each antibody (listed in Table S1) overnight at RT. Samples were washed with 0.1 M PBST, incubated with N-Histofine Simple Stain Mouse MAX PO (R) or (G) (Nichirei Biosciences) for 1 hr at 30°C, and then washed with 0.1 M PBS. Signal detection was carried out by incubating with 0.25 mg/ml 3,3'-diaminobenzidine and 0.006% H_2O_2 in 0.1 M PBS. Finally, samples were washed with 0.1 M PBS, then washed with distilled water, dehydrated with increasing concentrations of ethanol, cleared in xylene, and mounted on slides with Entellan new solution (Merck).

Monitoring circadian activity rhythms

Twelve-week-old male and female mice were housed in individual cages equipped with running wheels, and the cages were placed in a light-tight box (136.7 × 42.5 × 42.5 cm). Light in the box was provided by fluorescent lamps (white light: Panasonic FHF32EX-N-H, 4,150 lux at the top of the cage; UVA light: Philips TL-D 36W/08 low-pressure mercury vapour fluorescent lamp, peak wavelength 365 nm with half-bandwidth 13.9 nm) or a light-emitting diode (LED) (orange light: Beamtec LT40OS, straight tube LED, peak wavelength 602 nm with half-bandwidth 21.6 nm). The spectral profile of the UVA- and orange-light source is illustrated in Figure S1B. Light intensity was controlled using a neutral density filter (Fujifilm ND 0.9) and measured at the top of the cage (Monotech QTM-101). The UVA-light intensity was less than that observed under direct sunlight in Nagoya, Japan (~16 log photons cm^{-2} s^{-1}). Wheel-running activities were recorded using the Chronobiology Kit (Stanford Software Systems).

Circadian phase-shifting light pulses

Mice were kept under a white-light LD cycle (12/12-hr) for 2 weeks and transferred to constant darkness (DD). After 3 weeks in DD, mice were placed in a wire mesh cages (10 ×10 ×10 cm) and exposed to a 15-min UVA- or orange-light pulse at CT16, with CT12 defined as activity onset. Four

intensities of UVA- and two intensities of orange-light pulses were examined as shown in Figures 3C and 3D. Night-vision goggles (Ninox, Armasight) were used for all operations in the dark.

In situ hybridization of *Fos* mRNA

Since *Fos* expression peaks 30 min after stimulation (Radzioch et al., 1987), brains were collected 30 min after the beginning of the light pulse (log photon flux of 12.3) and rapidly frozen on dry ice. *Fos* mRNA was examined by *in situ* hybridization. Non-perfused, frozen sections (20-μm in thickness) were prepared using a cryostat (CM3050S, Leica Microsystems) and probed with ^{33}P-labeled oligonucleotides as previously described (Yoshimura et al., 2000). Four 45-mer oligonucleotide probes were designed for the mouse *Fos* gene (GenBank: NM_010234) and used as a mixture to increase the sensitivity. Hybridization of the probes was carried out overnight at 42°C. Two high-stringency washes were performed at 55°C. Samples were air-dried and exposed to BioMax MR Film (Eastman Kodak) for 4 weeks with ^{14}C-Standard slide (American Radiolabeled Chemicals). Densitometric quantification of the signal was performed using the Multi Gauge software (Fujifilm). The probe sequences were as follows:

5’- tcactgctcgttcgcggaaccgccggctctatccagtcttctcag - 3’
5’- tccagggaggccacagacatctcctctgggaagccaaggtcatcg - 3’
5’- atctggcacagagcgggaggtctctgagccactgggcctagatga - 3’
5’- ctggaggccagatgtggatgcttgcaagtccttgaggcccacagc - 3’

Statistical Analysis

All data are shown as the mean ± SEM. Statistical analyses were performed using one-way ANOVA, followed by Scheffé’s post-hoc test.

Supplemental References

Kojima, D., Mori, S., Torii, M., Wada, A., Morishita, R., and Fukada, Y. (2011). UV-sensitive photoreceptor protein OPN5 in humans and mice. PLoS One *6*, e26388.

Radzioch, D., Bottazzi, B., and Varesio, L. (1987). Augmentation of *c-fos* mRNA expression by activators of protein kinase C in fresh, terminally differentiated resting macrophages. Mol. Cell. Biol. *7*, 595–599.

Schalken, J.J., and De Grip, W.J. (1986). Enzyme-linked immunosorbent assay for quantitative determination of the visual pigment rhodopsin in total-eye extracts. Exp. Eye Res. *43*, 431–439.

Yoshimura, T., Suzuki, Y., Makino, E., Suzuki, T., Kuroiwa, A., Matsuda, Y., Namikawa, T., and Ebihara, S. (2000). Molecular analysis of avian circadian clock genes. Brain Res. Mol. Brain Res. *78*, 207–215.